26th ABCM International Congress of Mechanical Engineering
November 22-26, 2021. Florianópolis, SC, Brazil

COB-2021-COBEM2021-1954
NUMERICAL STUDIES OF FLOW AROUND FOUR CIRCULAR CYLINDERS IN SQUARE ARRANGEMENT

Paulo Vitor Reis Guilherme
Technological Center of Joinville
Federal University of Santa Catarina
Joinville, Santa Catarina 89219-600
Brazil
paulo.guilherme@grad.ufsc.br

Aline Peres Leal
Department of Naval and Oceanic Engineering
Polytechnic School of the University of São Paulo
São Paulo, São Paulo 05508-010
Brazil
aline.peresleal@usp.br

André Luís Condino Fujarra
Technological Center of Joinville
Federal University of Santa Catarina
Joinville, Santa Catarina 89219-600
Brazil
andre.fujarra@ufsc.br

Abstract. *Bodies submerged in water are rarely isolated. Instead of, the wake becoming from other bodies can strongly influence the response behavior, specially talking about amplitude of forces and movements. Offshore platforms as semisubmersibles have their four columns in square array and the study of motion in this case can be related to the platform movement induced by the flow, phenomenon known as flow-induced motion (FIM). The flow around four equal cylinders were analysed on this work, evaluating different relative distances between cylinders ($T/D = 2, 3, 4, 5, 6$) in CFD calculations. The study is treated in a way to present preliminary and reliable results for an array design, the flow is two-dimensional and at low Reynolds number ($Re = 100$), this approach proves to be advantageous in the selection of results and comparison with more elaborate simulations and experiments. Numerical calculations were carried out evaluating different number of cells and time steps in order to conduct uncertainty analysis, so the results are presented with their respective uncertainty intervals. The columns were evaluated in the stationary situation, i.e. no degree of freedom, where force coefficients and frequencies were analysed. It was noticed that the numerical results of this research presented good agreements with other numerical ones found in the literature, and symmetry results were found. The wake between the cylinders for $S \geq 4$ showed strong influence in the downstream response and some similarities related to the wake were found in comparison with two cylinders in tandem arrangement cases.*

Keywords: *square array, four cylinders, CFD, FIM, VIM*

1. INTRODUCTION

Flow-Induced Vibrations (FIV) on multiple bodies are of interest to many engineers and researchers, since the increasing of ocean structures operations, such as ocean platforms, risers, umbilical cables, and offshore wind turbines.

The improvement of computers and the development of Computational Fluid Dynamics (CFD) provided the ability to the resolution of more complex hydrodynamics problems applied to ocean structures. CFD became widely popular in the offshore industry especially due to the appearance of High-Performance Computing (HPC) (Darvishzadeh *et al.*, 2015). The CFD community can take advantage of the HPC benefits and investigate multiple bodies submerged into viscous fluids at various kinds of arrangements in detail and other more complex cases.

An interesting analysis is related to four identical and equally spaced cylinders, which is a popular subject due to the semi-submersible platform's applications. Gao *et al.* (2017) numerically studied the flow around four fixed square-

arranged identical circular cylinders at different Reynolds numbers ($100 < Re < 1000$) and different relative distances ($1.5 < S < 5$). They saw that the four cylinders are strongly affected by the spacing ratios and Reynolds numbers. Three flow patterns types were observed according to the space ratio variation (stable shielding flow pattern, wiggling shielding flow pattern, and vortex shedding flow pattern) and showed different responses in the cylinders, especially in drag and lift coefficients values.

Han *et al.* (2015) investigated a complex hydrodynamic case with FIV around four identical cylinders in square arrangement of $S = 5$ considering two degrees of freedom (2DOF) at low Reynolds numbers ($Re = 80$ and 100) and a range of reduced velocity ($3 < V_R < 14$). Each cylinder presented a mass ratio of $m^* = 6.0$ and was free to oscillate in in-line and transverse directions, so the columns presented different trajectory and forces responses, with maximum amplitudes occurrence for the two downstream cylinders. Different wake patterns were observed and the "dual-resonance" phenomenon occurred in this multi-body investigation, indicating the cylinders' synchronizations occurrence in both in-line and transverse directions. Further, numerical values for drag and lift coefficients were almost the same for the two upstream cylinders, and the same behavior happened for the downstream cylinders.

Zhang *et al.* (2019) conducted an experimental study of flow around an array of four square cylinders arranged in square configuration at $Re = 8000$ varying the cylinders' center-to-center pitch and the array orientation. The flow was broadly classified into three regimes (shielding, reattachment, and impinging) depending on the value of the center-to-center distance and array orientation. However, after a detailed approach, a new criterion was proposed to quantitatively classify the different flow regimes based on the average force coefficients.

Due to the importance of semi-submersible platforms and grouping of risers and their wide use in the offshore industry, this research aims to study the flow behavior involved in ocean platforms sustained by four equally stationary cylinders in square arrangements at low Reynolds number ($Re = 100$) at different relative distances ($S = 2$, 3, 4, 5, 6), multiples of the cylinders diameter.

2. NUMERICAL SIMULATION

The numerical calculations were conducted using OpenFOAM software v6, according to Greenshields (2018). For the stationary columns, the piso algorithm was applied. Each column was analyzed separately in terms of force coefficients, with the nomenclature according to Figure 1. The computational domain used is illustrated in Figure 2. The distance between columns varies from 2 to 6 diameters ($S = 2$, 3, 4, 5, and 6), leading to different domain sizes for each case. Due to the complexity of generating meshes with multiple bodies using the blockMesh tool, present in OpenFOAM, the four cylinders' meshes were created using an external tool.

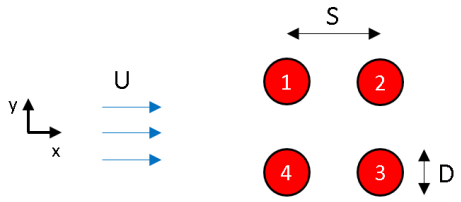

Figure 1. Configuration of the four-column arrays.

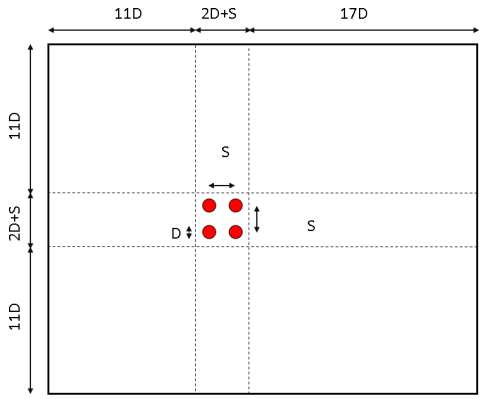

Figure 2. Computation domain related to the four-column arrays.

Figure 3 shows the space refinement of the region close to the columns array for $S = 2$. A higher refinement is required close to the cylinders in a way to reduce the discretization errors. Different numbers of cells and time steps were used, as will be related in the uncertainty analysis section.

In terms of simulation performance, it is important to evaluate the mesh quality, relating space and time discretization. The OpenFOAM software uses the Courant number and y^+ to assess the quality of numerical simulations.

The Courant number Co is a dimensionless relation that relates the time increment t, a particular cell size x, and the velocity magnitude of a fluid particle c in this cell. It indicates whether a portion of fluid travels through more than one cell per time interval. Thus, a Courant number smaller than one unit is very important, that is, $Co < 1$. It is represented by:

$$C_o = \frac{c\Delta t}{\Delta x} \tag{1}$$

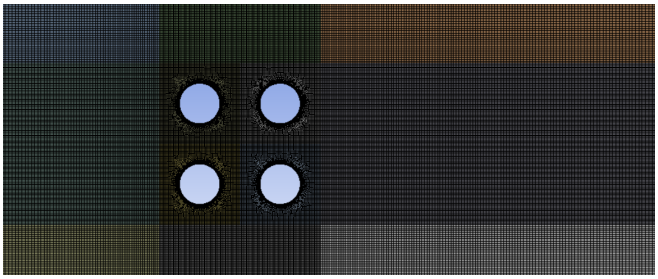

Figure 3. Four cylinders mesh, zoom in the columns array.

The y^+ parameter is a dimensionless distance used to describe the thickness of a mesh for a specific flow pattern, and it is important to determine the appropriate size of cells close to the domain walls. The wall is a region that presents high values of velocity gradients since there is a non-slip condition in the wall and a considerable flow velocity close to the wall.

The parameter y^+ defines in which layer the region close to the wall is (laminar boundary layer, turbulent boundary layer, or transition region), relating the friction velocity u, the distance between the wall and the cell closest to wall y and the kinematic viscosity of the fluid:

$$y^+ = \frac{u^* y}{\nu} \tag{2}$$

where the friction velocity relates to the wall shear stress τ_w and density of the fluid:

$$u^* \equiv \sqrt{\frac{\tau_w}{\rho}} \tag{3}$$

3. IMPORTANT PARAMETERS

It is usual to dimensionless parameters in CFD to make comparisons between the results, regardless of the simulation conditions. Tab. 1 presents some important parameters evaluated on this research and its respective descriptions.

Table 1. IMPORTANT DIMENSIONLESS PARAMATERS.

Parameters	Equation	Description
Reynolds number	$Re = UD/\nu$	It is defined as the ratio between inertial forces and viscous forces.
Strouhal number	$St = f_s D/U$	It is the dimensionless format of the vortex shedding frequency.
Drag coefficient	$C_D = F_D/0.5\rho U^2 A$	It is the dimensionless format of the force parallel to the flow direction.
Lift coefficient	$C_L = F_L/0.5\rho U^2 A$	It is the dimensionless format of the lift force, which is perpendicular to the flow direction.

4. DATA ANALYSIS

Post-processing analyzes were performed using Octave software. Based on the system's temporal records, data were obtained for drag and lift coefficients, and Strouhal number.

The statistic values for the force coefficients, drag (C_D) and lift (C_L) were calculated as the mean values, Eq. 4 and 5, and root mean square (rms) values, Eq. 6.

$$\overline{C_D} = \left[\sum_{i=1}^{N} C_{Di}\right]/N \tag{4}$$

$$\overline{C_L} = \left[\sum_{i=1}^{N} C_{Li}\right]/N \tag{5}$$

$$C_{L,rms} = \sqrt{\frac{1}{N}\sum_{i=1}^{N} C_{L_i}^2} \tag{6}$$

To calculate the vortex shedding frequencies, the temporal registers of the lift coefficient was taken into account. The Fast Fourier Transform (FFT) was used for the frequencies calculations.

Also, vorticity in the z-plane was observed through Paraview, an open-source visualization application and the main post-processing tool provided with OpenFOAM.

5. UNCERTAINTY ANALYSIS

The estimation of uncertainty through convergence analysis is an important study to evaluate how the simulation is reliable. Numerical uncertainties presented in this section were estimated based on the procedure presented by Eça and Hoekstra (2009); Eça *et al.* (2010), in a way to determine the exact solution.

In this procedure, three mesh sizes and five time steps were analyzed for each case considered in the numerical analysis. After carrying out these simulations, only the cases with Co and y^+ less than one were considered to calculate the uncertainty values.

For the stationary cylinders, uncertainty analysis were conducted for $S = 3$, where the frequencies and amplitudes were well defined.

The verification analysis was performed varying space and time discretizations. Three cells numbers and five time steps were chosen. Each time step is identified in a dimensionless format:

$$\tau_i = \Delta t_i / \Delta t_{min} \tag{7}$$

where Δt_i is the time step used in the simulation considered and Δt_{min} is the finest time step used in the calculations.

The grid is identified by:

$$h_i = \sqrt{\frac{N_{cells,max}}{N_{cells,i}}} \tag{8}$$

in which $N_{cells,max}$ is the number of cells in the finest grid and $N_{cells,i}$ is the number of cells in the case under analysis.

The values used to perform the uncertainty analysis are presented on Tab. 2.

Table 2. MESH AND TIME DISCRETIZATIONS FOR FOUR CYLINDERS IN SQUARE ARRANGEMENT OF $S = 3$.

Number of cells	h_i	time step	τ_i	$\Delta tU/D$
176823	1.0	2.5	1	0.0016064
176823	1.0	3	1.2	0.0048192
176823	1.0	4	1.6	0.0064256
176823	1.0	5	2	0.008032
176823	1.0	7.5	3	0.012048
46109	2.0	2.5	1	0.004016
46109	2.0	3	1.2	0.0048192
46109	2.0	4	1.6	0.0064256
46109	2.0	5	2	0.008032
46109	2.0	7.5	3	0.012048
19470	3.0	2.5	1	0.004016
19470	3.0	3	1.2	0.0048192
19470	3.0	4	1.6	0.0064256
19470	3.0	5	2	0.008032
19470	3.0	7.5	3	0.012048

There are three types of numerical errors: rounding, iteration, and discretization errors. Rounding errors are associated with computer precision but can be neglected through the use of double-precision, i.e., 15 digits.

Iteration errors are associated with the non-linearity of the equations solved by CFD. However, Eça and Hoekstra (2014) concluded that these errors can be neglected if low tolerances values less or equal to 10^{-5} were used for solving the systems of equations present in the CFD technique. Discretization errors occur due to the approximation made to transforming partial differential equations into a system of algebraic equations. These errors are the main sources of numerical errors and can be estimated through Richardson's extrapolation for transient regimes:

$$\delta_{RE} = \phi_i - \phi_0 = \alpha_x h_i^{p_x} + \alpha_t \tau_i^{p_t} \tag{9}$$

where h_i and τ_i are typical cell size and time step in the simulations; p_x and p_t are the observed orders of space and time discretization, respectively; α_x and α_t are constants of expansions; and, ϕ_0 is the estimated exact solution. According to Eq. 9, five unknowns should be calculated, requiring at least five simulations.

According to Eq. 9, five unknowns must be determined, and the Least Squares Method can be used for that. For flows in transient regimes, it is necessary to determine the observed orders of space and time discretization. Three conditions might occur:

- If $p > 0$: there is a possible monotonic convergence;
- If $p < 0$: there is a possible monotonic divergence;
- If there is no value for p: there is a possible oscillatory convergence or divergence.

Then, it is possible to estimate with 95% of confidence Eça and Hoekstra (2009) the following range:

$$\phi_i - U(\phi_i) \leq \phi_{exact} \leq \phi_i + U(\phi_i) \tag{10}$$

where $U(\phi_i)$ is the uncertainty of the property ϕ_i obtained from the estimated discretization error.

6. RESULTS

This section presents the results for four stationary cylinders in square arrangement. The results are discussed in terms of the obtained numerical values and vorticity field. The square arrangement is also compared with a single stationary cylinder, based on Guilherme and Fujarra (2020), and with two cylinders in tandem arrangement, based on Leal *et al.* (2021).

6.1 Uncertainty Results

It is shown in Tab. 3 the uncertainty results of the finest mesh and smallest time step simulation for the coefficients of the fixed case at $S = 3$, considering the results with 4 decimal places . It was observed higher uncertainty values for $C_{L,rms}$ of the Cylinder 2, 3 and 4, as well as for $\overline{C_D}$ of the Cylinder 2, however, the values are still acceptable. Strouhal number coefficients are very stable and present low uncertainty values.

Table 3. NUMERICAL UNCERTAINTY RESULTS FOR STATIONARY CYLINDERS IN SQUARE ARRANGEMENT AT $Re = 100$ AND $S = 3$, FOR THE MOST REFINED MESH AND SMALLEST TIME STEP.

Cylinder	Item	ϕ_{exact}	ϕ_1	$\% U$	$\phi_1 - U$	$\phi_1 + U$
Cylinder 1	$\overline{C_D}$	1.3583	1.3594	0.1%	1.3580	1.3608
	$\overline{C_L}$	0.1517	0.1514	0.2%	1.5111	0.1516
	St	0.1420	0.1411	0.9%	0.1400	0.1422
Cylinder 2	$\overline{C_D}$	0.2705	0.2562	16.7%	0.2133	0.2991
	$\overline{C_L}$	0.0791	0.0830	13.9%	0.0701	0.0959
	St	0.1420	0.1411	0.9%	0.1400	0.1422
Cylinder 3	$\overline{C_D}$	0.2633	0.2572	3.1%	0.2496	0.2648
	$\overline{C_L}$	-0.0765	-0.0840	18.4%	-0.0990	-0.0690
	St	0.1421	0.1411	0.9%	0.1398	0.1424
Cylinder 4	$\overline{C_D}$	1.3582	1.3593	0.2%	1.3560	1.3626
	$\overline{C_L}$	-0.1591	-0.1498	18.4%	-0.1778	-0.1218
	St	0.1421	0.1411	0.9%	0.1398	0.1424

6.2 Four stationary cylinders in square arrangement

Fig. 4 represents mean drag coefficients results in the stationary case varying the relative distance, as well as the results found according to Lam *et al.* (2008) and Gao *et al.* (2017). Cylinders 1 and 4 presented close drag coefficients values, and the same occurrence was observed for cylinders 2 and 3. The present results also showed good agreements with the literature for each one of the four evaluated cylinders. The upstream cylinders (cyl. 1 and cyl. 4) presented low variation in drag coefficient according S increasing. However, the downstream cylinders (cyl. 2 and cyl. 3) presented an abrupt increase in drag coefficient at $S = 4$, which is probably associated with the change in the flow behavior. This abrupt variation happens due to the change in the flow behavior at $S = 4$, as it will be seen in the vorticity field analyzed ahead.

It is possible to see graphically that the uncertainty is the biggest for the cyl.4, and this interval covers the values found in the literature.

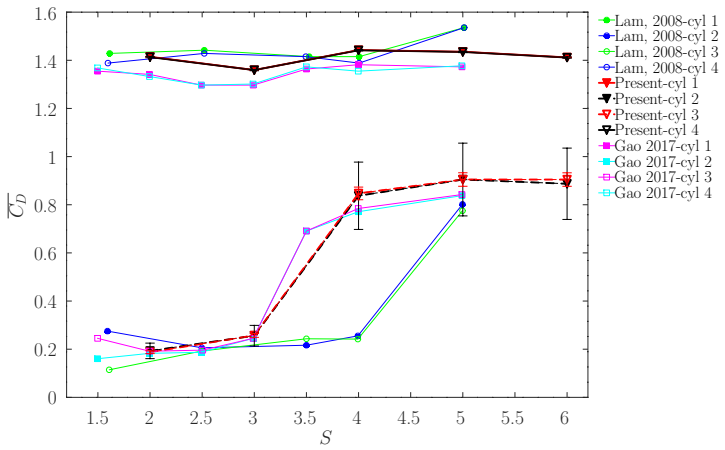

Figure 4. Drag coefficients results from literature and found in the present work.

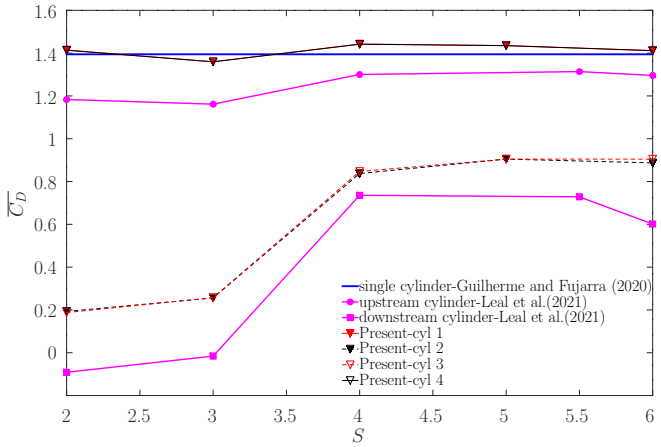

Figure 5. Drag coefficients results for different configurations.

Symmetry results were found for lift coefficients according to Fig. 6, i.e., the upstream cylinders (cyl. 1 and cyl. 4) presented same magnitude, but opposite directions. A similar occurrence was observed for the downstream cylinders (cyl. 2 and cyl. 3). The upstream cylinders presented the highest values of lift coefficients and all the cylinders showed a seeming convergence to zero according to the increasing of S, what is expected for a single cylinder, where the interaction with the other cylinders does not present interference.

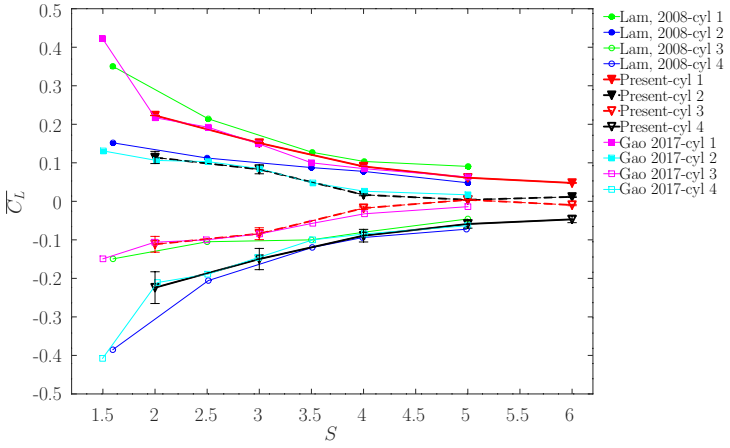

Figure 6. Lift coefficients results from literature and found in the present work.

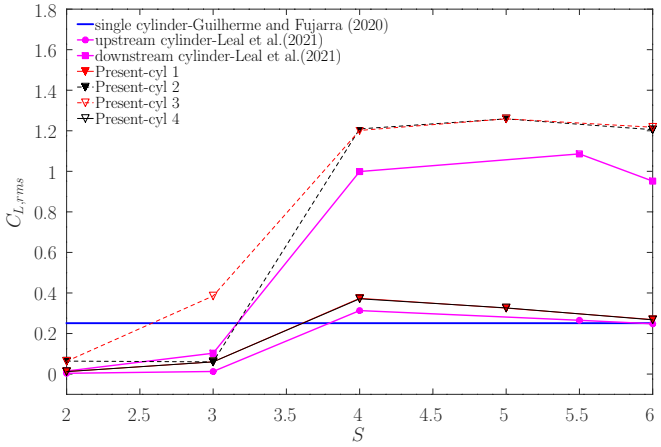

Figure 7. Lift rms coefficients results for different configurations.

Fig. 4 shows Strouhal number in function of S. It was observed that for $S \geq 3$, all the four cylinders have the same St values. Further, St increases slightly in the range of $2 \leq S \leq 4$, indicating a vortex shedding frequency increasing as S increases. In the range of $S > 4$, St presents low variations and it is almost constant.

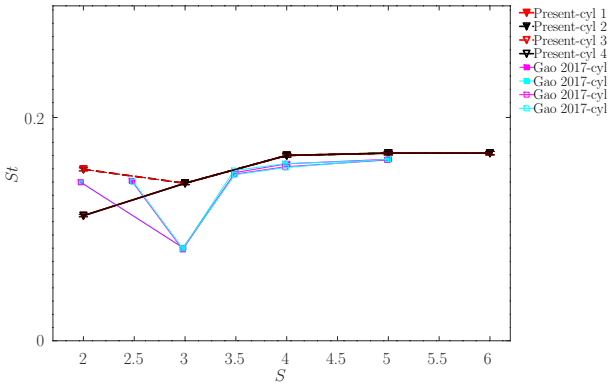

Figure 8. Strouhal number results from literature and found in the present work.

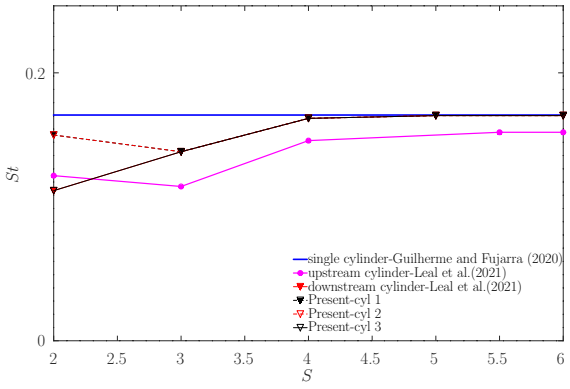

Figure 9. Strouhal number results for different configurations.

Some results above might be explained by the vorticity field analysis, according to Fig. 10, 11, 12, 13, and 14, which represents the vortex shedding for $S = 2$, 3, 4, 5, and 6, respectively. It was observed a wake of vortex between the upstream cylinders and downstream cylinders (first wake) for $S \geq 4$ and also a wake soon after the downstream cylinders (second wake); however, none wake was formed between upstream and downstream cylinders for $S < 4$ due to the vortex merging before the vortex shedding of the downstream cylinder, caused by the relative high proximity between the bodies.

The presence of a wake between the bodies might be lead St at higher values for all cylinders in the square arrangement, showing a seemingly computational convergence according to St increasing. Furthermore, it was observed that the second wake presented higher magnitude values of vorticity for $S \geq 4$. These occurrences might be lead the downstream cylinders to a suddenly increasing in $\overline{C_D}$ and St, especially. Moreover, as observed by Gao *et al.* (2017) and also on this research, the two vortices generated between cyl. 1 and 4 pass through the gap between cyl. 2 and 3.

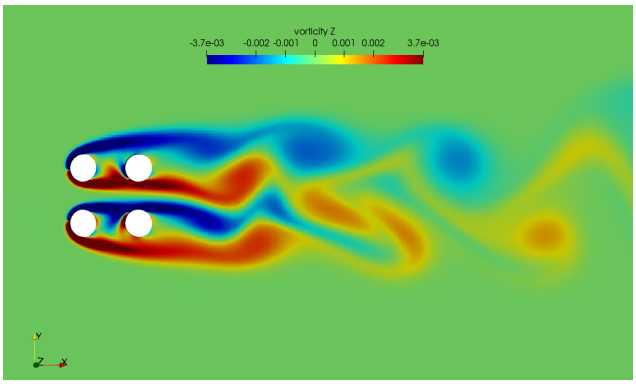

Figure 10. Vorticity field for $S = 2$.

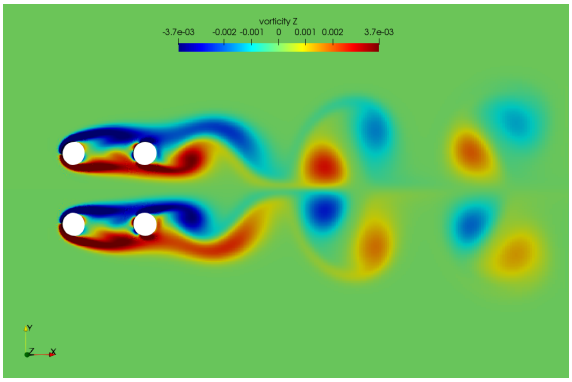

Figure 11. Vorticity field for $S = 3$.

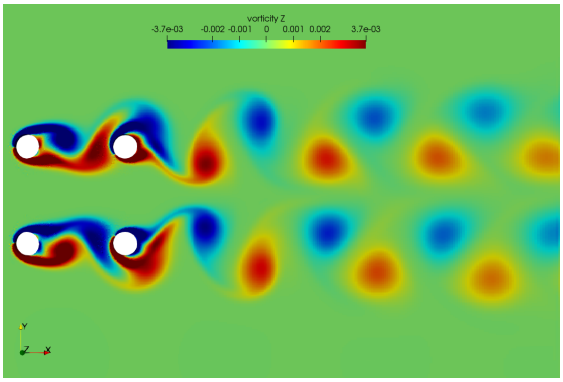

Figure 12. Vorticity field for $S = 4$.

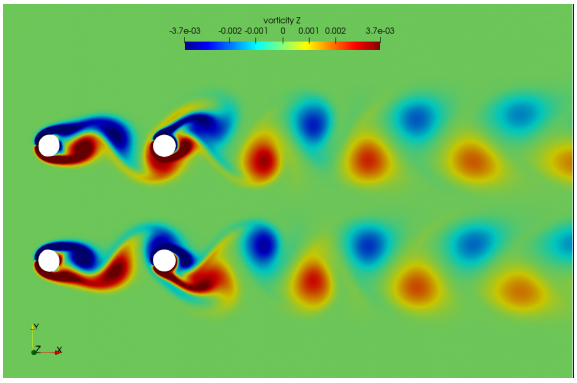

Figure 13. Vorticity field for $S = 5$.

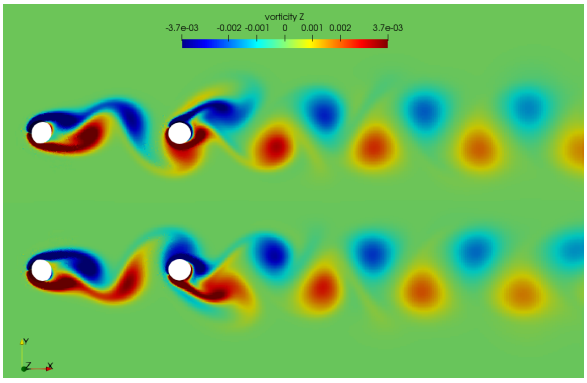

Figure 14. Vorticity field for $S = 6$.

6.3 Single cylinder case comparision

This subsection presents comparisons between four cylinders in square arrangement results with the single cylinder case, performed by Guilherme and Fujarra (2020), according to Fig. 5, 7 and 9.

The upstream cylinders of the square arrangement case (cyl. 1 and 4) presented qualitative similar behaviors of a single cylinder case for all the studied relative distances in terms of the drag coefficient. The drag coefficient of the singular case, about $\overline{C_D} = 1.3945$, showed strong computational proximity with the upstream cylinders of the square arrangement. However, the downstream cylinders (cyl. 2 and 3) presented much lower values of $\overline{C_D}$ in comparison of a single cylinder. This may be occurred due to the wake interference between the cylinders (first wake). This behavior was also exposed by the experimental studies of Gonçalves *et al.* (2017), at Re = 250,000.

The lift coefficient, about $C_{L,rms} = 0.2510$, and Strouhal number, about $St = 0.1685$, for the single case, showed strong computational proximity with the upstream cylinders of the square arrangement for $S \geq 4$. This may be happened due to the not interference of the downstream cylinders' vortex shedding to the upstream ones in the range of $S \geq 4$. No interference occurs between bottom (cyl. 3 and 4) and top (cyl. 1 and 2) bodies in this range too, and this happens due to

the gap presence between top and bottom cylinders. Some differences occurred at $S < 4$ for $C_{L,rms}$ and St, indicating a lower vortex shedding frequency for all the cylinders.

6.4 Two cylinders in tandem arrangement case comparison

According to Fig. 5, 7 and 9, it was observed that the pair of the two top cylinders in square arrangement, as well as the pair of the two bottom cylinders, presented qualitative similar behaviors in comparison with the cylinders in tandem arrangement performed by Leal *et al.* (2021). Both arrangements also presented wake interference and a change in flow behavior for $S \geq 4$, called critical distance.

Related to the upstream body of two sections in tandem arrangement, $\overline{C_D}$ and $C_{L,rms}$ presented lower values for the upstream square arrangement cylinders, although relatives close values. It was also noticed that Strouhal numbers are slightly higher for the upstream square arrangement bodies in all the studied distances, indicating a higher vortex emission frequency. The difference of the downstream cylinders of the square arrangement is a little bigger than the downstream cylinders of the two cylinders in tandem arrangement in terms of $\overline{C_D}$ and $C_{L,rms}$.

7. CONCLUSIONS

Two-dimensional simulations of four stationary cylinders in square arrangement at $Re = 100$ were performed using OpenFOAM software.

It was noticed symmetry results, i.e., cyl. 1 and 4 (upstream cylinders) presented close values of $\overline{C_D}$, $C_{L,rms}$ and St, and the same symmetry occurrence was observed for cyl. 2 and 3 (downstream cylinders). All the results presented good agreements with those numerical ones found in the literature.

It was also observed the existence of a wake between the pair of top cylinders, as well as the pair of bottom cylinders, for $S \geq 4$. This wake caused changes in flow behavior and in the downstream results, especially.

The upstream cylinders of the square arrangement case (cyl. 1 and 4) presented qualitative similar behaviors of a single cylinder in terms of the drag coefficient, but some differences were found for lift coefficient and Strouhal number due to the wake interference. A similar wake was noticed in Leal *et al.* (2021) studies related to two cylinders in tandem arrangement, and the same phenomena was observed.

Finally, this study contributed to the literature involving FIV analysis around four cylinders in square arrangement, presenting good agreements after comparisons with numerical results in the literature and, enabling comparison with other types of arrangement, thus expanding the analyses. This research also showed that OpenFOAM presents strong performances on complex fluid structural interactions.

8. REFERENCES

Darvishzadeh, T., Sari, A. *et al.*, 2015. "Cfd applications in offshore engineering". In *Offshore Technology Conference*. Offshore Technology Conference.

Eça, L. and Hoekstra, M., 2009. "Evaluation of numerical error estimation based on grid refinement studies with the method of the manufactured solutions". *Computers & Fluids*, Vol. 38, No. 8, pp. 1580–1591.

Eça, L., Vaz, G. and Hoekstra, M., 2010. "A verification and validation exercise for the flow over a backward facing step". In *Fifth European Conference on Computational Fluid Dynamics*. pp. 14–17.

Eça, L. and Hoekstra, M., 2014. "A procedure for the estimation of the numerical uncertainty of cfd calculations based on grid refinement studies". *Journal of computational physics*, Vol. 262, pp. 104–130.

Gao, Y.y., Yin, C.s., Zhang, H.q., Yang, K., Zhao, X.z. and Sun, Z., 2017. "Numerical study on flow around four square-arranged cylinders at low reynolds numbers". *Mathematical Problems in Engineering*, Vol. 2017.

Gonçalves, R.T., Hirabayashi, S. and Suzuki, H., 2017. "Experimental study on flow around an array of four cylinders with different section geometries". In *International Conference on Offshore Mechanics and Arctic Engineering*. American Society of Mechanical Engineers, Vol. 57649, p. V002T08A018.

Greenshields, C.J., 2018. "Openfoam user guide version 6". *The OpenFOAM Foundation*.

Guilherme, P.V.R. and Fujarra, A.L.C., 2020. "Numerical investigation on vortex-induced motions of offshore structures of varying mass ratios at re=100". *Proceedings of the 28th International Congress on Waterborne Transportation, Shipbuilding and Offshore*.

Han, Z., Zhou, D., He, T., Tu, J., Li, C., Kwok, K.C. and Fang, C., 2015. "Flow-induced vibrations of four circular cylinders with square arrangement at low reynolds numbers". *Ocean Engineering*, Vol. 96, pp. 21–33.

Lam, K., Gong, W. and So, R., 2008. "Numerical simulation of cross-flow around four cylinders in an in-line square configuration". *Journal of Fluids and Structures*, Vol. 24, No. 1, pp. 34–57.

Leal, A.P., Guilherme, P.V.R. and Fujarra, A.L.C., 2021. "Numerical investigation on flow-induced vibrations of circular sections in tandem arrangement varying relative distance". *Proceedings of the ASME 2021 40th InternationalConference on Ocean, Offshore and Arctic Engineering*.

Zhang, J., Chen, H., Zhou, B. and Wang, X., 2019. "Flow around an array of four equispaced square cylinders". *Applied Ocean Research*, Vol. 89, pp. 237–250.